

Making Universal Policies Universal

Niklas Hoepner
University of Amsterdam
Amsterdam, Netherlands
n.r.hopner@uva.nl

David Kuric
University of Amsterdam
Amsterdam, Netherlands
d.kuric@uva.nl

Herke van Hoof
University of Amsterdam
Amsterdam, Netherlands
h.c.vanhoof@uva.nl

ABSTRACT

The development of a generalist agent capable of solving a wide range of sequential decision-making tasks remains a significant challenge. We address this problem in a cross-agent setup where agents share the same observation space but differ in their action spaces. Our approach builds on the universal policy framework, which decouples policy learning into two stages: a diffusion-based planner that generates observation sequences and an inverse dynamics model that assigns actions to these plans. We propose a method for training the planner on a joint dataset composed of trajectories from all agents. This method offers the benefit of positive transfer by pooling data from different agents, while the primary challenge lies in adapting shared plans to each agent’s unique constraints. We evaluate our approach on the BabyAI environment, covering tasks of varying complexity, and demonstrate positive transfer across agents. Additionally, we examine the planner’s generalisation ability to unseen agents and compare our method to traditional imitation learning approaches. By training on a pooled dataset from multiple agents, our universal policy achieves an improvement of up to 42.20% in task completion accuracy compared to a policy trained on a dataset from a single agent¹.

KEYWORDS

Diffusion Models, Cross-Agent Learning, Inverse Dynamics, Task Planning, Instruction Following, Generalist Agent

1 INTRODUCTION

The challenge of developing a generalist agent capable of addressing a diverse range of sequential decision-making tasks remains an open problem [37]. Successfully solving this challenge holds the potential to eliminate the need for task-specific engineering and retraining, while also enhancing performance through positive transfer between tasks [45, 50]. Given the vast differences in observation and action spaces across tasks, most general agents are still developed for specific domains such as robotic manipulation [4, 45], web agents [10], computer control [51], or embodied navigation [55]. However, image-based observations offer a common ground for many sequential decision-making tasks, even when the corresponding action spaces vary significantly. Image observations are prevalent in contexts such as gameplay [17, 29], robotic control [33], and web or computer interfaces [10, 46], among others. Training a policy that can solve tasks that have environment observations in a unified format, such as images, is an important step towards creating a generalist agent. In this work, we move closer to this goal by developing a policy capable of controlling agents that share a common observation space but have different action spaces.

Recently, universal policies [14] have emerged as a promising framework for learning multi-task policies through text guided video generation. This method is composed of two stages: first, a conditional diffusion model is trained to translate task descriptions into image-observation sequences; then, an inverse dynamics model is applied to map these sequences to the corresponding actions. A key advantage of this approach is the ability to pretrain the video generation model on vast datasets of instruction-video pairs [15, 31, 41] or directly leveraging text-to-video foundation models [8, 18] as the planner. Additionally, the visual nature of the generated plans enhances interpretability by allowing inspection of the proposed solutions. Another potential advantage, which has not been investigated yet, lies in creating a shared planner for multiple agents, which can be paired with agent-specific inverse dynamics models to produce a policy capable of controlling all agents.

We explore this problem in a cross-agent setting where a group of agents shares the same observation space but operates with different action spaces. For each agent, there exists a small dataset of instruction-trajectory pairs. However, a single agent-specific dataset alone does not contain enough demonstrations such that training an agent-specific instruction-following policy through imitation learning on top of it would yield a policy capable of adequately solving the tasks for this agent. Our objective is to develop a policy that can successfully solve tasks for all agent types by pooling data from individual agents. To achieve this, we extend the universal policy framework to learn a policy on the combined dataset capable of controlling all the different agents.

The primary challenge lies in ensuring that the diffusion-based planner accounts for the varying capabilities of each agent (see Figure 1); otherwise, it may generate observation sequences that cannot be labelled via the agent-specific inverse dynamics model, leading to unpredictable behavior. On the other hand, this approach offers the potential for positive transfer, as the planner is exposed to a larger number of examples during training, which could lead to improved policies for each agent type. We investigate different methods for conditioning the planner on agent type information and assess their ability to generalise to unseen agents. In summary, our contributions are as follows:

- (1) Extending the universal policy framework to train a policy on a dataset consisting of trajectories from a diverse set of agents, capable of controlling all of them.
- (2) Comparing different approaches to condition the shared planner on agent type information and studying their ability to generalise to unseen agents.

2 RELATED WORK

We begin with an overview of approaches to training a generalist agent—a policy capable of solving a wide range of sequential decision-making tasks. Next, we discuss algorithms developed for

¹<https://github.com/NikeHop/UniversalPolicies>

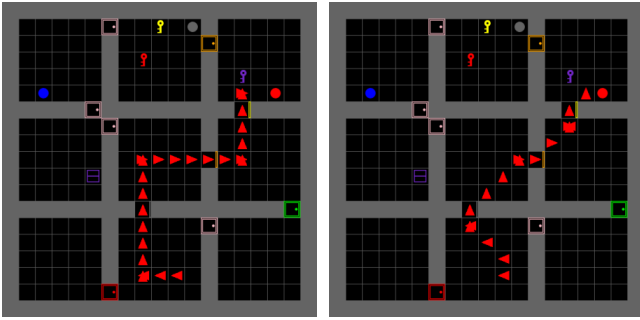


Figure 1: Example for the different plans the shared planner needs to generate for different agent types. The agent on the left follows the standard action space (forward, turn left, turn right) in the BabyAI environment while the agent on the right can move to any of the surrounding squares and turn right.

cross-embodiment policy learning (CEPL) as the data setup is similar to ours. Finally, we review work focused on using diffusion models to learn control policies.

2.1 Building generalist agents

The GATO agent [37] represents the policy trained across the most diverse set of sequential decision-making tasks. It accomplishes this by mapping various action and observation spaces into tokens, which are then processed and predicted by a transformer architecture [47]. The effectiveness of this approach relies on the presence of generalizable patterns within the tokenized trajectory data, enabling positive transfer. A bottleneck in training general policies is the need to train policies from scratch which is computationally intensive. To address this, researchers have begun integrating multi-modal foundation models [5, 13, 34] into their policies [23, 53, 57]. An example is the RT-2 model [57], which translates robotic actions into tokens and co-finetunes PaLI-X [5] and Palm-E [13] vision-language models using robotic trajectory data. Similarly, our adaptation of the universal policy approach can be combined with text-to-video foundation models [8, 18].

2.2 Cross Embodiment Policy Learning

In robotics where data collection is costly, the community created increasingly larger datasets of task-trajectory pairs [9, 28, 30, 33]. One possibility to scale the amount of available data quickly is to pool data over robotic agents with different embodiments. For example the Open X-Embodiment (OXE) dataset pools several existing robotic manipulation datasets [33]. Learning over different embodiments comes with the challenge of learning a policy that needs to be able to handle different action and observation spaces.

While training agent-agnostic policies is not a new goal [21], the embodiment gap has widened significantly, such that robot behaviour is even learned from human demonstrations [35, 52]. To address this challenge, two main approaches have emerged. The first maps different observation and action spaces of various embodiments into token sequences with a uniform structure, allowing them to be processed by a shared transformer [12, 45]. The second

focuses on learning a joint latent space that aligns different embodiments within a common embedding space, enabling policy learning over this latent representation [48, 52].

Our own data setup mirrors the OXE dataset as it pools agent-specific datasets from different agents. However, in the case of the OXE dataset, agents have varying observation spaces in addition to their differing action spaces. To learn a policy that can control a diverse set of agents we follow the universal policy approach [14] and frame policy learning as learning a generative model for observation sequences in combination with agent-specific inverse dynamics models. We further show that training a shared diffusion planner achieves greater positive transfer than imitation learning approaches with separate policy heads for each agent [12, 45].

2.3 Policy Learning with Diffusion

The recent success of diffusion models in learning generative models for images [38, 39], audio [54], and videos [18] has extended to policy learning [7, 14, 16, 24, 27]. These models can learn policies by either mapping states to action distributions [7, 27] or modelling probability distributions over agent trajectories as sequences of state-action pairs [24]. In the latter approach, a trajectory is sampled based on a given task description and initial observation and then executed by the agent. Another approach proposed by Du et al. [14], known as universal policies, learns a generative model over observation sequences conditioned on natural language instructions. Instead of generating action sequences directly, it generates observation sequences, which are then labelled with appropriate actions using an inverse dynamics model. This method not only outperforms imitation learning baselines [3] and trajectory-based diffusion models [24] but also shows potential for integration with text-to-video foundation models. Additionally, it enhances interpretability by allowing inspection of the generated observation sequences. If agents share a common observation space, the diffusion-based planner for universal policies can be trained using trajectories from agents with varying capabilities. However, at test time, the generated plans must conform to the specific agent’s capability constraints. To the best of our knowledge, we are the first to explore diffusion-based generative modeling of observation sequences on datasets containing trajectories from agents with heterogeneous action spaces.

3 METHODOLOGY

We begin by extending the theoretical framework underlying universal policies called Unified Predictive Decision Process (UDPD) [14] to be compatible with the cross agent setting. Then we introduce the data setup assumed for our approach, followed by a description how we implement the shared diffusion planner that can be conditioned on different types of agent information.

3.1 CA-UDPD

A cross agent UDPD (CA-UDPD) is a tuple $G = (N, X, C, H, p)$, where N is a set of agents, X represents the observations space for all agents, C is a space of task descriptions, H the time horizon and $p(\cdot|x_0, c, k) : X \times C \times N \rightarrow \Delta(X^H)$ a conditional probability distribution over H -step observation sequences that depends on the current observation x_0 , the task c and the agent k executing the task.

Here $\Delta(Z)$ denotes a probability distribution over the space Z . The set of task descriptions as well as the observation space can take different forms. For example C can be the set of all natural language instructions and X the set of all RGB-images. The UDPD framework was introduced to address common challenges encountered when modelling real-world problems with MDPs [2] and to shift focus on observation generation as a solution technique to learning policies. Instead of using a reward function, UDPD employs a more general set of task descriptions, recognizing that reward functions are often difficult to define in a way that consistently leads to the desired behaviour [11]. Additionally, the action space and transition dynamics are not explicitly modelled but are captured within the conditional probability distribution over observation sequences. For a more detailed comparison between MDPs and UDPDs, we refer readers to the original paper [14]. For control an agent-specific policy $\pi_k : X^H \rightarrow \Delta(A_k^{H-1})$ that maps observation sequences to a probability distribution over a sequence of actions from the agents action space A_k needs to be learned for every agent type k .

3.2 Problem Setup

For each agent $n \in N$, we have a dataset D_n consisting of M_n instruction-trajectory pairs, denoted as $D_n = \{(c_i, x_{1:t_i}, a_{i:t_i})\}_{i=1}^{M_n}$, where $c_i \in C$ represents the instruction for the i -th sample and $a_{i:t_i}$ represents the action sequence the agent chose to complete the task, generating the observation sequence $x_{1:t_i} \in X^{t_i}$. Regarding the relation of the observation space of the different agents we consider two extreme cases. In the first case, all agents share the same observation space, i.e., $X_n = X_m = X \quad \forall n, m \in N$. In the second case, the observation spaces are entirely disjoint, such that $X_n \cap X_m = \emptyset \quad \forall n, m \in N$. In the latter scenario, the agent identifier is inherently embedded in the observation x_t , allowing the planner p to identify the agent from the observation x_0 it is conditioned on and plan accordingly. Both scenarios are plausible, i.e. for example in the case of robotic manipulation [33] the image from the end-effector cameras would not let the planner identify which agent to plan for, while the static cameras will often show the agent the planner controls. We pool the individual datasets D_n to obtain a larger mixture dataset $D = \{(c_i, x_{1:t_i}, a_{i:t_i}, n_i)\}_{i=1}^M$, where $n_i \in N$ is the agent id of the i -th sample and $M = \sum_{n=1}^N M_n$ is the total number of trajectories aggregated over all datasets.

3.3 Universal Cross Agent Policy

The goal is to train the conditional observation sequence generator $p(\cdot|x_0, c, k)$ on the mixture dataset D , leading to a Universal Cross Agent Policy (UCAP). Instead of generating the complete observation sequence $x_{1:t_i}$ we sample random windows of size 4 and take the first timestep to be the starting observation x_0 , i.e. $p(\cdot|x_0, c, k)$ plans the next three timesteps for agent k following instruction c starting in x_0 . In contrast to previous work we do not apply temporal super resolution, i.e first generating a coarse video plan that is refined in a second step [14]. We estimate p using a conditional diffusion model. Diffusion models perturb data samples by gradually adding noise at different scales, then learn to reverse this process to recover the original data. New samples are generated by starting with noise and iteratively applying the learned reverse process to approximate the data distribution [19, 43].

We follow the ODE formulation from Karras et al. [26]. Let $p_{\text{data}}(x)$ be the data distribution and $p(x; \sigma)$ be the perturbed data distribution obtained by adding i.i.d Gaussian noise with standard deviation σ to it, i.e. $p(\tilde{x}; \sigma) = \int p_{\text{data}}(x) p_{\sigma}(\tilde{x}|x) dx$, where $p_{\sigma}(\tilde{x}|x) = N(\tilde{x}|x, \sigma)$ [44]. Given a continuous time noise schedule $\sigma(t)$, the solution to the following probabilistic flow ODE:

$$dx = -\dot{\sigma}(t)\sigma(t)\nabla_x \log p(x; \sigma(t))dt \quad (1)$$

has marginals corresponding to the noise perturbed data distribution with noise $\sigma(t)$, i.e $x_t \sim p(x_t, \sigma(t))$ [26]. If we have an estimate of the time dependent score function $\nabla_x \log p(x; \sigma(t))$ we can sample from the noise distribution $x_{t_0} \sim N(0, \sigma(t_0)I)$ and use ODE solvers [1] to turn the noise into samples from the data distribution. Following Karras et al. [26] this can be done by estimating a denoising function D_{θ} for different noise scales σ via the loss:

$$L(\theta) = \mathbb{E}_{x \sim p_{\text{data}}} \mathbb{E}_{n \sim N(0, \sigma I)} \|D_{\theta}(x + n; \sigma) - x\|_2^2, \quad (2)$$

where the denoising function D_{θ} and the score function are related via $\nabla_x \log p(x; \sigma) = (D(x; \sigma) - x)/\sigma^2$. At test time we then apply a sampler based on Heun’s method [1, 26] to generate observation sequences from noise.

Following [26], we condition the denoising network D_{θ} , on the conditioning information, i.e. the starting observation x_0 , the natural language instruction c and the agent information k to train a conditional diffusion model. The natural language instruction is embedded via a variant of the T5 model [36] and then added to the noise vector. Following Du et al. [14] we condition on the starting observation by concatenating it along the channel dimension for each timestep of the noise perturbed input. We could not find any benefit from classifier-free guidance [20] and set the guidance weight to zero. Next we describe different ways to condition the denoising network D_{θ} on agent information.

Agent ID: For each agent type a random embedding serves as the agent id and is added to the noise embedding in the same manner as the instruction embedding. For example in case of robotic manipulation [33] the planner would be conditioned on an embedding for each robot type (Franka Emika Panda, Sawyer, xArm, etc.). Since there is no relation between the ID and the capabilities of the agent, this type of conditioning cannot generalise to unseen agents with unseen IDs.

Action Space Representation: If the action space is discrete and partly shared, one can represent the action space via a binary vector $v \in \{0, 1\}^{|A|}$, where A is the union of all action agent-specific action spaces. If $v_i = 1$ the agent is capable of action i . To condition the denoising network D on this action space representation, we embed v via a linear layer and add it to the noise embedding. This way of conditioning can potentially generalise to new agent types that have unseen action combinations, as the actions themselves have previously been encountered.

Example Trajectory: Similar to the ability of LLM’s [25, 34] to perform in-context learning [32, 49], we can condition the planner on example observation sequences of the agent acting. If trained with a large enough number of different agent types and examples, it potentially generalizes to unseen agents by providing an example video of the novel agent’s capabilities. However, taking a random subsequence of frames from a video of the agent acting as context is unlikely to be informative about the agent. For example in the

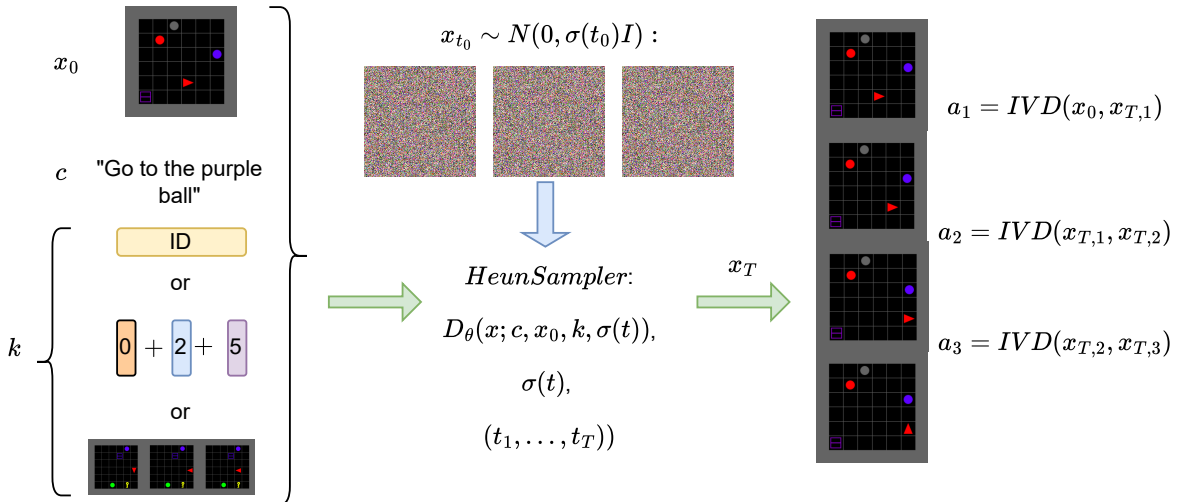


Figure 2: Overview of how actions are generated by UCAP. Given the starting observation x_0 , the instruction c and the different types of agent information k to condition on, a Heun Sampler is applied for T steps to generate an observation sequence of 3 timesteps from noise. Two consecutive observations are then labelled via the inverse dynamics model to produce the action sequence the agent will take.

BabyAI environment [6] shown in Figure 1, sampling a subsequence where an agent only moves forward is uninformative of whether the agent can move diagonally or not. Conditioning on longer example videos increases the likelihood of the random video to be informative but also increase computational cost. In case of a discrete action space one option is to demonstrate each action the agent is capable of once. We condition on the resulting example video by concatenating it to the front of the noise perturbed sample along the time dimension.

Given a planner that can generate observation sequences, a set of inverse dynamics models needs to be trained for each agent type to label the sequences with the corresponding actions. An inverse dynamics model for agent $n \in N$ is a function that takes two consecutive observations and maps them into the agent-specific action space $IVD_n : X \times X \rightarrow A_n$. Given an observation sequence that is labelled with actions we can sample consecutive observation pairs and train the IVD to predict the correct action via the cross entropy loss. Since inverse dynamics models are sample efficient to learn they can be easily trained on the smaller agent specific dataset D_n . An overview of how a universal policy selects its actions can be seen in Figure 2. The details of the network architectures and training parameters for the conditional diffusion planner as well as the inverse dynamics models can be found in Appendix B.

4 EXPERIMENTS

We begin with outlining the experimental environment that facilitates the creation of agents with varying action spaces. Next, we investigate whether training on a pooled dataset, composed of trajectories from agents of different types, results in positive transfer. Additionally, we examine the impact of conditioning the planner

on the different types of agent information presented in Section 3.3. In the sections that follow, we compare the performance of UCAP against imitation learning baselines tailored to our data setup and conclude with ablations that investigate the performance of UCAP in the case of disjoint observation spaces, the effect of planning granularity on performance and the effect of number of agent types on generalisation performance.

4.1 Environment

We choose BabyAI [6] as the evaluation environment since it is easily modifiable and offers a range of tasks with varying complexity. In the BabyAI environment an agent needs to navigate a gridworld to complete different tasks ranging from navigating to objects to opening doors with keys. The environment state can either be represented as a gridworld or an RGB image. Here we choose the gridworld representation as it is computationally more efficient. The environment state is fully observable. An agent's performance is evaluated by the percentage of tasks completed correctly over 512 episodes. The standard action space consists of six actions (turn left, turn right, move forward, pickup, drop, toggle). We extend the action space to a total of 18 actions (e.g. turn 180 degrees, move diagonal, etc). To create different action spaces for different agents we mask out actions that are not available for the specific agent. In total we create eight agent types. An overview of the different agent types and their capabilities can be found in Table 1. A summary of all the possible actions can be found in Appendix A. The mixture dataset D is created by pooling the demonstrations of agents 0-5 (see Table 1). The other two agents are left out to test generalisation of models to unseen agents. We refer to agents whose datasets are included in the pooled dataset as In-Distribution

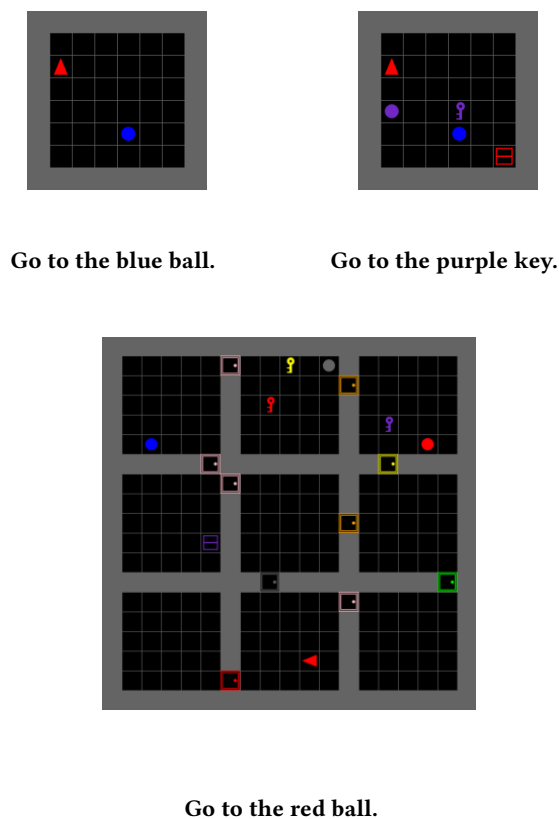


Figure 3: Example environment observations from GoToObj (top left), GoToDistractor (top right) and GoToDistractor-Large (bottom). The agent is the red triangle.

(ID) agents, while agents whose datasets are not included are called Out-of-Distribution (OOD) agents. We test the universal policy approach on the following three environment instances ²:

GoToObj: The agent needs to navigate to the only object in the environment. The object can be a key, box, or ball, and comes in one of six different colours. This task does not require any natural language task instructions as the task is always the same. The environment observations have size $8 \times 8 \times 3$ and the trajectory length is at most 25 timesteps.

GoToDistractor: The same environment as the GoTo environment but with 3 distractor objects added. Now the natural language instruction is necessary to understand to which object to navigate.

GoToDistractorLarge: The goal of the environment is the same as in the GoToDistractor environment. However the agent is now in one of nine rooms that are connected via doors and the environment contains 7 distractor objects. The environment observation is of size $22 \times 22 \times 3$ and the maximum trajectory length is at most 100 timesteps. An image representation of the different environment observations can be seen in Figure 3.

Table 1: Overview of the different action spaces. The mixture of datasets used for training is derived from the ID agent types 0-5 and the OOD agent types are 6-7.

AS	Description
0	Standard: All actions of the standard action space are allowed.
1	No left: The agent cannot turn left.
2	No right: The agent cannot turn right.
3	Diagonal: The agent can additionally move a diagonal step forward either to the right or left.
4	WSAD: The agent can move one field to the right left, up and down and turns into the direction it moves.
5	Dir8: The agent can move to any of the eight surrounding fields and turn right.
6	Left-Right: The agent can go left and right and turn right.
7	All Diagonal: The agent can go to all the diagonal cells and turn right.

4.2 Positive Transfer

Positive transfer occurs if UCAP outperforms on average the universal policies trained for a specific agent type on the agent specific dataset. In order to investigate whether positive transfer occurs we perform the following steps:

- (1) Train a universal policy for a single agent on a small agent-specific dataset for each agent type.
- (2) Train a universal policy on the mixture of small datasets (UCAP). Here we train a policy for each type of agent information from Section 3.3 (Mixture-Example, Mixture-AgentID, Mixture-ActionSpace) and one UCAP that is not conditioned on any agent information (Mixture).
- (3) Train a universal policy for a each agent type on an agent-specific dataset equal in size to the mixture dataset.

The performances of the universal policies trained on the small and larger dataset serves as anchor to evaluate the amount of positive/negative transfer that occurs. The policy generated by training on the large dataset is an upper bound to the amount of transfer we can expect. Any performance improvement above the policy trained on the smaller dataset is a sign of positive transfer, and any performance decrease is a sign of negative transfer. For the two smaller environments we perform the analysis for all agent types. For the GoToDistractorLarge environment, we only do the analysis for the standard action space, i.e. no single agent policies are trained for the other agent types to save computational resources.

In Figure 4 we can see the performance of the different universal policies in the three environments for the standard agent. To save compute we only train UCAP conditioned on the action space encoding for the GoToDistractorLarge environment since it worked best in the smaller environments. For all environments UCAP conditioned on any type of the agent representation shows positive transfer, where conditioning on a representation of the action space works best and conditioning on examples has the worst mean task completion rate. One possible reason for the weaker performance

²<https://github.com/Farama-Foundation/Minigrid>

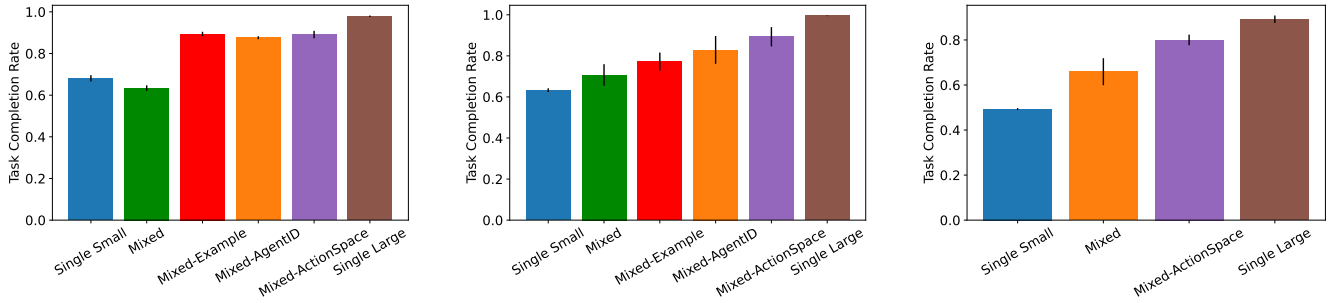


Figure 4: Mean task completion rate for a range of UCAP models on the three evaluation environments GoToObj (left), GoToDistractor (middle), GoToDistractorLarge (right) for an agent with the standard action space which belongs to the ID agent set. All results are averaged over 4 random seeds and error bars indicate the standard error.

when conditioning on examples is their higher dimensionality compared to agent ID and action space encodings, such that it takes more samples to estimate the conditional probability distribution correctly. The results for the diffusion planner without agent information are mixed showing positive transfer in the more complex environment and negative transfer in the simplest environment. One potential reason is that for more complex environments the agent will encounter unseen distractor goal combinations if not enough training data is present. Having observed these combinations even in trajectories from other agents can be beneficial for the planning performance. Therefore it can be beneficial to train on the mixture dataset even if no agent information is present. However, conditioning on agent information offers large performance benefits.

Table 2 shows the task completion rates of UCAP conditioned on different action space information, averaged across agent types, for both ID and OOD agents. For ID agents, the results mirror those from the standard action space, except that the planner without agent conditioning does not exhibit negative transfer in the GoToObj environment. In GoToObj, transfer effects depend on the agent type: more general action spaces allow for better execution of planner-proposed actions, leading to positive transfer. For instance, in GoToObj, the mean task completion rate drops from 0.827 ± 0.023 to 0.617 ± 0.016 for agents that cannot turn right but increases from 0.705 ± 0.058 to 0.731 ± 0.026 for agents that can move diagonally. For OOD agents, UCAP conditioned on examples or action space information shows no generalization. A possible reason is the limited agent diversity, causing conditioned information to be treated as ID. The planner may struggle to correlate actions in video examples with those in demonstrations due to insufficient variability in agent types. This hypothesis will be further examined in an ablation study in subsection 4.4.

4.3 Baselines

We compare UCAP to imitation learning baselines adapted to learning from multiple smaller datasets from different agents. The policy architecture for all imitation learning baselines consists of a convolutional stack followed by an MLP [22]. Policies are trained to predict the agent’s next action given a state sampled from the expert

Table 2: Mean task completion rate averaged over all ID and OOD agents respectively for different UCAP models in the GoToObj environment and GoToDistractor environment. All results are averaged over 4 seeds and brackets contain standard errors. The best performing models for ID agents as well as OOD agents are in bold, where models trained on large individual datasets are excluded.

Model	GoToObj-Env	
	ID Agents	OOD Agents
Single Agent Small	0.753(0.009)	0.657(0.005)
Mixed	0.760(0.003)	0.396(0.014)
Mixed Example	0.857(0.005)	0.453(0.010)
Mixed Agent-ID	0.850(0.004)	0.261(0.055)
Mixed ActionSpace	0.850(0.009)	0.494(0.021)
Single Agent Large	0.915(0.002)	0.970(0.004)
GoToDistractor-Env		
	ID Agents	OOD Agents
Single Agent Small	0.627(0.003)	0.650(0.007)
Mixed	0.726(0.047)	0.315(0.017)
Mixed Example	0.795(0.042)	0.404(0.024)
Mixed Agent-ID	0.843(0.060)	0.193(0.019)
Mixed ActionSpace	0.892(0.053)	0.541(0.034)
Single Agent Large	0.995(0.001)	0.996(0.002)

demonstrations. More details on the architecture and hyperparameters can be found in Appendix B.3. We implement the following approaches:

Imitation Learning (IL): We train a single agent policy on the small and large dataset. Again the performance on the large dataset serves as an upper bound of imitation learning, while the performance on the smaller dataset serves as a threshold to whether we observe positive or negative transfer.

IL - Union of Action Spaces: A common way of handling different actions spaces is to form the union over all agents action spaces [56]. The model receives a one-hot encoded vector representing the agent ID, which is concatenated with the output of

Table 3: Average task completion rate averaged over all ID agents and OOD agents respectively for imitation learning (IL) baselines in comparison to universal policies (UP) trained on single agent datasets and mixture datasets. Results are averaged across four random seeds and standard errors are in brackets. The naming of the model consists of first the method name, then the dataset trained on and thirdly an indicator whether finetuning is performed after training. The best performing method that has access to only the small individual agent datasets is in bold.

Model	GoToObj-Env		GoToDistractor-Env	
	ID Agents	OOD Agents	ID Agents	OOD Agents
IL - Single Agent Small	0.638(0.010)	0.390(0.017)	0.504(0.006)	0.514(0.018)
IL Union of Action Spaces - Mixture	0.763(0.022)	0.030(0.004)	0.812(0.005)	0.026(0.002)
IL Union of Action Spaces - Mixture - Finetuned	0.880(0.003)	0.705(0.009)	0.803(0.029)	0.7028(0.031)
IL Agent Heads - Mixture	0.818(0.008)	0.012(0.001)	0.801(0.018)	0.016(0.005)
IL Agent Heads - Mixture - Finetuned	0.827(0.003)	0.771(0.008)	0.811(0.037)	0.742(0.044)
UCAP - Action Space	0.850(0.009)	0.494(0.021)	0.892(0.053)	0.541(0.034)
UCAP - Action Space - Finetuned	0.839(0.007)	0.788(0.011)	0.872(0.046)	0.904(0.039)
IL - Single Agent Large	0.907(0.003)	0.955(0.009)	0.953(0.006)	0.944(0.001)

the convolutional embedding stack. If the agent chooses an invalid action there is no change to the environment state.

IL - Agent Heads: Following the approach of the Octo-policy [45] we employ different agent heads but keep the same convolutional backbone, i.e. for each agent a separate MLP is trained to predict the action the agent of the specific type needs to take.

We implement finetuned versions of the imitation learning baselines, where the policy is first trained on the large mixture dataset and then finetuned on smaller agent-specific datasets. For comparison, we also finetune a universal policy without agent information after training it on the mixture dataset.

Table 3 shows the imitation learning baselines compared to the universal policy conditioned on an action space encoding. Both imitation learning variants show positive transfer, with task completion rates improving when trained on the mixture dataset instead of the small single-agent dataset in both environments. As expected, without finetuning, the imitation learning baselines cannot generalize to OOD agents. For policies with varying agent heads, a new agent requires predicting actions via an untrained head, while the imitation learning baseline receives an unseen agent ID as input. The universal policy conditioned on action space information outperforms both baselines in both environments, with a larger performance gap in the more complex environment. None of the methods generalize to OOD agents. The standard approach to handle this is finetuning on a small dataset from the unseen agent [45]. The finetuned universal policy outperforms the finetuned imitation learning baselines, with the gap widening in more complex environments. This suggests it is easier to finetune the observation sequence planner than to learn a new agent head or adapt a large action space distribution to a new one-hot encoding.

4.4 Ablations

4.4.1 Disjoint Observation Spaces. As mentioned in Section 3.2 the observation space of different agents does not necessarily need to overlap, i.e. the observation itself contains information on the agent type. The planner could potentially leverage this information to adjust the plan of the agent accordingly. To emulate this setting in the BabyAI environment, we give each agent type a different

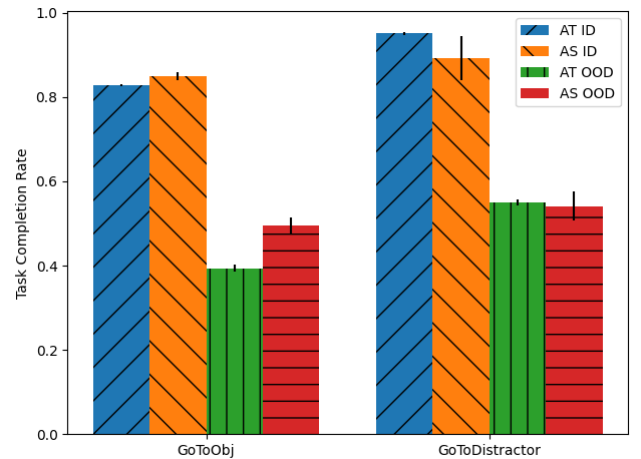


Figure 5: Mean task completion rate over all ID and OOD agent types in the GoToObj and GoToDistractor environment for the universal policy trained on a mixture of dataset with a visual agent type (AT) and without a visual agent-type but conditioned on an encoding of the action space (AS). Results are averaged over 4 random seeds and error bars indicate standard errors.

colour and train the universal policy on a newly created mixed dataset where agents are identifiable via their colour. In Figure 5 we compare the results to the best UCAP model with uniformly coloured agents in the GoToObj and GoToObjDistractor environment. The planner successfully leverages the colour information and reaches a task completion rate comparable or higher than the UCAP conditioned on an action space encoding. As expected the planner does not generalise to OOD agents with an OOD colour.

4.4.2 Planning Granularity. An alternative strategy to handle differing action spaces is to plan at a coarser timestep, where the planner suggests the next goal state, and each agent’s goal-conditioned

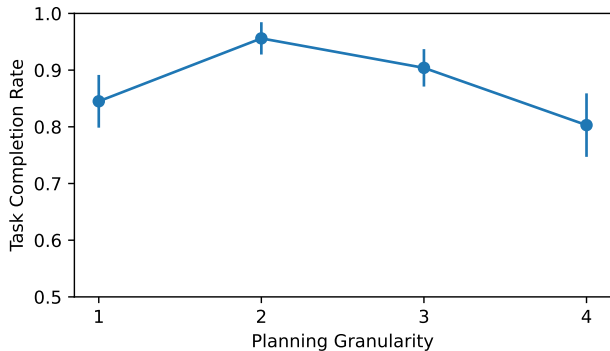


Figure 6: Task completion rate for diffusion planners with different planning granularities trained on the mixture dataset.

Model	GoToDistractor-Env	
	ID Agents	OOD Agents
UCAP 1-Step	0.726(0.024)	0.315(0.09)
UCAP 2-Step	0.885(0.011)	0.918(0.010)

Table 4: Average task completion rate for UCAP with different planning granularity trained on the mixture dataset. Experiments are run over 4 seeds and numbers in brackets indicate standard error.

policy chooses the action to move from the current state to the proposed goal. This approach has the benefit that the generated plans do not need to conform with the agents capabilities at a timestep level, but transfers the responsibility from the planner to the agent-specific goal-conditioned policies. Compared to learning an inverse dynamics model, developing a local goal-conditioned policy typically requires more data due to the increased complexity of the mapping. Here, local refers to the fact that the goal is reachable within a few timesteps.

To test this, we trained the diffusion planner on subsampled trajectories in the GoToDistractor environment, selecting the start and end states along with every n -th timestep, and trained a goal-conditioned policy through imitation learning by sampling start and goal states from the agent-specific datasets. First, we evaluated only the planner’s performance across different planning granularity levels using an oracle policy, which moved the agent to each planner-suggested goal state. In Figure 6 we can see that the best planning performance is reached when planning for two timesteps. Evaluating the 2-step planner with the agent-specific goal-conditioned policies shows also an improved task completions rate compared to combining a 1-step planner with agent-specific IVD models (see Table 4). Notably, the performance on the OOD agents is on par with the performance for the ID agents as the 2-step planner cannot propose impossible actions for agents anymore.

4.4.3 Increased Agent Diversity. One possible reason why conditioning on either an encoding of the action space or trajectory examples fails to generalize to OOD agents is the limited diversity of agents in the training set. With only six different agents, it may

Model	OOD Agents
UCAP Action Space	0.906(0.010)
UCAP Example	0.611(0.012)

Table 5: Average task completion rate for UCAP trained on the mixed dataset with different conditioning information for OOD agents. Experiments are run over 4 seeds and numbers in brackets indicate standard error.

be difficult to learn the correlation between conditioning information and the possible actions in the trajectory to be reconstructed. To address this, we created a dataset for the GoToDistractor environment, consisting of trajectories from 6,595 different agents by combining the 18 possible actions in various ways. Notably, the dataset size remains unchanged compared to the previous setup. As shown in Table 5, this increased diversity improves the generalisation performance of both conditioning methods. The mean task completion rate increases from 0.494 ± 0.021 to 0.906 ± 0.010 when conditioned on the action space encoding and from 0.453 ± 0.10 to 0.611 ± 0.012 when conditioned on example trajectories.

5 LIMITATIONS

While we observed positive transfer from training on a pooled dataset of different agents, it is unclear whether this transfer will hold when environment observations vary more significantly, such as in the OXE dataset [33], which includes observations from diverse robotic manipulators. Future work should attempt to scale the approach to larger datasets with heterogenous A drawback of using the diffusion planner is the increased training and inference time. Convergence requires approximately 40 times more updates compared to imitation learning, and the sampler needs 128 neural function evaluations versus just one for imitation learning. Techniques like progressive distillation [40] and consistency models [42] improve sampling speed with minimal loss in generative ability.

6 CONCLUSION

We showed that it is possible to leverage the universal policy approach [14] to train a diffusion based planner that generates observations sequences for agents with different capabilities. Training the planner on a pooled dataset from all agent types leads to an improved universal policy compared to training on the smaller agent specific datasets alone. The performance of the planner can be improved by conditioning on agent specific information such as the encoding of the action space or example observation sequences. Independent of the agent information the planner is conditioned on generalisation to OOD agents without finetuning remains a challenging task, where potential solution strategies include increased agent diversity and planning at a higher granularity level. Future work should extend the approach to agents with heterogenous observation spaces [12, 45] and scale it to more complex environments [33].

ACKNOWLEDGMENTS

This research was (partially) funded by the Hybrid Intelligence Center, a 10-year programme funded by the Dutch Ministry of Education, Culture and Science through the Netherlands Organisation for Scientific Research, <https://hybrid-intelligence-centre.nl>. This work used the Dutch national e-infrastructure with the support of the SURF Cooperative using grant no. EINF-6630.

REFERENCES

- [1] Uri M. Ascher and Linda R. Petzold. 1998. *Computer methods for ordinary differential equations and differential-algebraic equations*. SIAM.
- [2] Richard Bellman. 1958. Dynamic Programming and Stochastic Control Processes. *Inf. Control*, 1, 3 (1958), 228–239. [https://doi.org/10.1016/S0019-9958\(58\)80003-0](https://doi.org/10.1016/S0019-9958(58)80003-0)
- [3] Anthony Brohan, Noah Brown, Justice Carbajal, Yevgen Chebotar, Joseph Dabis, Chelsea Finn, Keerthana Gopalakrishnan, Karol Hausman, Alexander Herzog, Jasmine Hsu, Julian Ibarz, Brian Ichter, Alex Irpan, Tomas Jackson, Sally Jesmonth, Nikhil J. Joshi, Ryan Julian, Dmitry Kalashnikov, Yuheng Kuang, Isabel Leal, Kuang-Huei Lee, Sergey Levine, Yao Lu, Utsav Malla, Deeksha Manjunath, Igor Mordatch, Ofir Nachum, Carolina Parada, Jodilyn Peralta, Emily Perez, Karl Pertsch, Jormell Quiambao, Kanishka Rao, Michael S. Ryoo, Grecia Salazar, Panag R. Sanketi, Kevin Sayed, Jaspiar Singh, Sumedh Sontakke, Austin Stone, Clayton Tan, Huong T. Tran, Vincent Vanhoucke, Steve Vega, Quan Vuong, Fei Xia, Ted Xiao, Peng Xu, Sichun Xu, Tianhe Yu, and Brianna Zitkovich. 2023. RT-1: Robotics Transformer for Real-World Control at Scale. In *Robotics: Science and Systems XIX, Daegu, Republic of Korea, July 10-14, 2023*, Kostas E. Bekris, Kris Hauser, Sylvia L. Herbert, and Jingjin Yu (Eds.). <https://doi.org/10.15607/RSS.2023.XIX.025>
- [4] Chi-Lam Cheang, Guangzeng Chen, Ya Jing, Tao Kong, Hang Li, Yifeng Li, Yuxiao Liu, Hongtao Wu, Jiafeng Xu, Yichu Yang, et al. 2024. GR-2: A Generative Video-Language-Action Model with Web-Scale Knowledge for Robot Manipulation. *arXiv preprint arXiv:2410.06158* (2024).
- [5] Xi Chen, Josip Djolonga, Piotr Padlewski, Basil Mustafa, Soravit Changpinyo, Jialin Wu, Carlos Riquelme Ruiz, Sebastian Goodman, Xiao Wang, Yi Tay, Siamak Shakeri, Mostafa Dehghani, Daniel Salz, Mario Lucic, Michael Tschannen, Arsha Nagrani, Hexiang Hu, Mandar Joshi, Bo Pang, Ceslee Montgomery, Paulina Pietrzyk, Marvin Ritter, A. J. Piergiovanni, Matthias Minderer, Filip Pavetic, Austin Waters, Gang Li, Ibrahim Alabdulmohsin, Lucas Beyer, Julien Amelot, Kenton Lee, Andreas Peter Steiner, Yang Li, Daniel Keysers, Anurag Arnab, Yuanzhong Xu, Keran Rang, Alexander Kolesnikov, Mojtaba Seyedhosseini, Anelia Angelova, Xiaohua Zhai, Neil Houlsby, and Radu Soricut. 2023. PaLI-X: On Scaling up a Multilingual Vision and Language Model. *CoRR abs/2305.18565* (2023). <https://doi.org/10.48550/ARXIV.2305.18565>
- [6] Maxime Chevalier-Boisvert, Dzmitry Bahdanau, Salem Lahlou, Lucas Willems, Chitwan Saharia, Thien Huu Nguyen, and Yoshua Bengio. 2019. BabyAI: A Platform to Study the Sample Efficiency of Grounded Language Learning. In *7th International Conference on Learning Representations, ICLR 2019, New Orleans, LA, USA, May 6-9, 2019*. OpenReview.net. <https://openreview.net/forum?id=rjEXCo0cYX>
- [7] Cheng Chi, Siyuan Feng, Yilun Du, Zhenjia Xu, Eric Cousineau, Benjamin Burchfiel, and Shuran Song. 2023. Diffusion Policy: Visuomotor Policy Learning via Action Diffusion. In *Robotics: Science and Systems XIX, Daegu, Republic of Korea, July 10-14, 2023*, Kostas E. Bekris, Kris Hauser, Sylvia L. Herbert, and Jingjin Yu (Eds.). <https://doi.org/10.15607/RSS.2023.XIX.026>
- [8] Joseph Cho, Fachrina Dewi Puspitasari, Sheng Zheng, Jingyao Zheng, Lik-Hang Lee, Tae-Ho Kim, Choong Seon Hong, and Chaoning Zhang. 2024. Sora as an AGI World Model? A Complete Survey on Text-to-Video Generation. *CoRR abs/2403.05131* (2024). <https://doi.org/10.48550/ARXIV.2403.05131>
- [9] Sudeep Dasari, Frederik Ebert, Stephen Tian, Suraj Nair, Bernadette Bucher, Karl Schmeckpeper, Siddharth Singh, Sergey Levine, and Chelsea Finn. 2019. RoboNet: Large-Scale Multi-Robot Learning. In *3rd Annual Conference on Robot Learning, CoRL 2019, Osaka, Japan, October 30 - November 1, 2019, Proceedings (Proceedings of Machine Learning Research, Vol. 100)*, Leslie Pack Kaelbling, Danica Kragic, and Komei Sugiura (Eds.). PMLR, 885–897. <http://proceedings.mlr.press/v100/dasari20a.html>
- [10] Xiang Deng, Yu Gu, Boyuan Zheng, Shijie Chen, Samuel Stevens, Boshi Wang, Huan Sun, and Yu Su. 2023. Mind2Web: Towards a Generalist Agent for the Web. In *Advances in Neural Information Processing Systems 36: Annual Conference on Neural Information Processing Systems 2023, NeurIPS 2023, New Orleans, LA, USA, December 10 - 16, 2023*, Alice Oh, Tristan Naumann, Amir Globerson, Kate Saenko, Moritz Hardt, and Sergey Levine (Eds.). http://papers.nips.cc/paper_files/paper/2023/hash/5950bf290a1570ea401bf98882128160-Abstract-Datasets_and_Benchmarks.html
- [11] Lauro Langosco di Langosco, Jack Koch, Lee D. Sharkey, Jacob Pfau, and David Krueger. 2022. Goal Misgeneralization in Deep Reinforcement Learning. In *International Conference on Machine Learning, ICML 2022, 17-23 July 2022, Baltimore, Maryland, USA (Proceedings of Machine Learning Research, Vol. 162)*, Kamalika Chaudhuri, Stefanie Jegelka, Le Song, Csaba Szepesvári, Gang Niu, and Sivan Sabato (Eds.). PMLR, 12004–12019. <https://proceedings.mlr.press/v162/langosco22a.html>
- [12] Ria Doshi, Homer Walke, Oier Mees, Sudeep Dasari, and Sergey Levine. 2024. Scaling Cross-Embodied Learning: One Policy for Manipulation, Navigation, Locomotion and Aviation. *CoRR abs/2408.11812* (2024). <https://doi.org/10.48550/ARXIV.2408.11812>
- [13] Danny Driess, Fei Xia, Mehdi S. M. Sajjadi, Corey Lynch, Aakanksha Chowdhery, Brian Ichter, Ayzan Wahid, Jonathan Tompson, Quan Vuong, Tianhe Yu, Wenlong Huang, Yevgen Chebotar, Pierre Sermanet, Daniel Duckworth, Sergey Levine, Vincent Vanhoucke, Karol Hausman, Marc Toussaint, Klaus Greff, Andy Zeng, Igor Mordatch, and Pete Florence. 2023. PaLM-E: An Embodied Multimodal Language Model. In *International Conference on Machine Learning, ICML 2023, 23-29 July 2023, Honolulu, Hawaii, USA (Proceedings of Machine Learning Research, Vol. 202)*, Andreas Krause, Emma Brunskill, Kyunghyun Cho, Barbara Engelhardt, Sivan Sabato, and Jonathan Scarlett (Eds.). PMLR, 8469–8488. <https://proceedings.mlr.press/v202/driess23a.html>
- [14] Yilun Du, Sherry Yang, Bo Dai, Hanjun Dai, Ofir Nachum, Josh Tenenbaum, Dale Schuurmans, and Pieter Abbeel. 2023. Learning Universal Policies via Text-Guided Video Generation. In *Advances in Neural Information Processing Systems 36: Annual Conference on Neural Information Processing Systems 2023, NeurIPS 2023, New Orleans, LA, USA, December 10 - 16, 2023*, Alice Oh, Tristan Naumann, Amir Globerson, Kate Saenko, Moritz Hardt, and Sergey Levine (Eds.). http://papers.nips.cc/paper_files/paper/2023/hash/1d5b923ad716a43be5c0d3023cb82d0-Abstract-Conference.html
- [15] Kristen Grauman, Andrew Westbury, Eugene Byrne, Zachary Chavis, Antonino Furnari, Rohit Girdhar, Jackson Hamburger, Hao Jiang, Miao Liu, Xingyu Liu, Miguel Martin, Tushar Nagarajan, Ilija Radosavovic, Santhosh Kumar Ramakrishnan, Fiona Ryan, Jayant Sharma, Michael Wray, Mengmeng Xu, Eric Zhongcong Xu, Chen Zhao, Siddhant Bansal, Dhruv Batra, Vincent Cartillier, Sean Crane, Tien Do, Morrie Doulaty, Akshay Erappalli, Christoph Feichtenhofer, Adriano Fragomeni, Qichen Fu, Abrahm Gebreselasie, Cristina González, James Hillis, Xuhua Huang, Yifei Huang, Wenqi Jia, Weslie Khoo, Jáchym Kolár, Satwik Kotur, Anurag Kumar, Federico Landini, Chao Li, Yanghao Li, Zhenqiang Li, Kartikeya Mangalam, Raghava Modhugu, Jonathan Munro, Tullie Murrell, Takumi Nishiyasu, Will Price, Paola Ruiz Puentes, Merey Ramazanov, Leda Sari, Kiran Somasundaram, Audrey Southerland, Yusuke Sugano, Ruijie Tao, Minh Vo, Yuchen Wang, Xindi Wu, Takuma Yagi, Ziwei Zhao, Yunyi Zhu, Pablo Arbeláez, David Crandall, Dima Damen, Giovanni Maria Farinella, Christian Fuegen, Bernard Ghanem, Vamsi Krishna Ithapu, C. V. Jawahar, Hanbyul Joo, Kris Kitani, Haizhou Li, Richard A. Newcombe, Aude Oliva, Hyun Soo Park, James M. Rehg, Yoichi Sato, Jianbo Shi, Mike Zheng Shou, Antonio Torralba, Lorenzo Torresani, Mingfei Yan, and Jitendra Malik. 2022. Ego4D: Around the World in 3, 000 Hours of Egocentric Video. In *IEEE/CVF Conference on Computer Vision and Pattern Recognition, CVPR 2022, New Orleans, LA, USA, June 18-24, 2022*. IEEE, 18973–18990. <https://doi.org/10.1109/CVPR52688.2022.01842>
- [16] Xianfan Gu, Chuan Wen, Weirui Ye, Jiaming Song, and Yang Gao. 2024. Seer: Language Instructed Video Prediction with Latent Diffusion Models. In *The Twelfth International Conference on Learning Representations, ICLR 2024, Vienna, Austria, May 7-11, 2024*. OpenReview.net. <https://openreview.net/forum?id=qHGgNyQk31>
- [17] William H. Guss, Brandon Houghton, Nicholay Topin, Phillip Wang, Cayden Codel, Manuela Veloso, and Ruslan Salakhutdinov. 2019. MineRL: A Large-Scale Dataset of Minecraft Demonstrations. In *Proceedings of the Twenty-Eighth International Joint Conference on Artificial Intelligence, IJCAI-19. International Joint Conferences on Artificial Intelligence Organization, 2442–2448*. <https://doi.org/10.24963/ijcai.2019/339>
- [18] Jonathan Ho, William Chan, Chitwan Saharia, Jay Whang, Ruiqi Gao, Alexey A. Gritsenko, Diederik P. Kingma, Ben Poole, Mohammad Norouzi, David J. Fleet, and Tim Salimans. 2022. Imagen Video: High Definition Video Generation with Diffusion Models. *CoRR abs/2210.02303* (2022). <https://doi.org/10.48550/ARXIV.2210.02303>
- [19] Jonathan Ho, Ajay Jain, and Pieter Abbeel. 2020. Denoising Diffusion Probabilistic Models. In *Advances in Neural Information Processing Systems 33: Annual Conference on Neural Information Processing Systems 2020, NeurIPS 2020, December 6-12, 2020, virtual*, Hugo Larochelle, Marc'Aurelio Ranzato, Raia Hadsell, Maria-Florina Balcan, and Hsuan-Tien Lin (Eds.). <https://proceedings.neurips.cc/paper/2020/hash/4c5bfcfec8584af0d967f1ab10179ca4b-Abstract.html>
- [20] Jonathan Ho and Tim Salimans. 2022. Classifier-Free Diffusion Guidance. *CoRR abs/2207.12598* (2022). <https://doi.org/10.48550/ARXIV.2207.12598>
- [21] Wenlong Huang, Igor Mordatch, and Deepak Pathak. 2020. One Policy to Control Them All: Shared Modular Policies for Agent-Agnostic Control. In *Proceedings of the 37th International Conference on Machine Learning, ICML 2020, 13-18 July 2020, Virtual Event (Proceedings of Machine Learning Research, Vol. 119)*. PMLR, 4455–4464. <http://proceedings.mlr.press/v119/luang20d.html>

- [22] David Yu-Tung Hui, Maxime Chevalier-Boisvert, Dzmitry Bahdanau, and Yoshua Bengio. 2020. BabyAI 1.1. *CoRR* abs/2007.12770 (2020). arXiv:2007.12770 <https://arxiv.org/abs/2007.12770>
- [23] Brian Ichter, Anthony Brohan, Yevgen Chebotar, Chelsea Finn, Karol Hausman, Alexander Herzog, Daniel Ho, Julian Ibarz, Alex Irpan, Eric Jang, Ryan Julian, Dmitry Kalashnikov, Sergey Levine, Yao Lu, Carolina Parada, Kanishka Rao, Pierre Sermanet, Alexander Toshev, Vincent Vanhoucke, Fei Xia, Ted Xiao, Peng Xu, Mengyuan Yan, Noah Brown, Michael Ahn, Omar Cortes, Nicolas Sievers, Clayton Tan, Sichun Xu, Diego Reyes, Jarek Rettinghouse, Jornell Quiambao, Peter Pastor, Linda Luu, Kuang-Huei Lee, Yuheng Kuang, Sally Jesmonth, Nikhil J. Joshi, Kyle Jeffrey, Rosario Jauregui Ruano, Jasmine Hsu, Keerthana Gopalakrishnan, Byron David, Andy Zeng, and Chuyuan Kelly Fu. 2022. Do As I Can, Not As I Say: Grounding Language in Robotic Affordances. In *Conference on Robot Learning, CoRL 2022, 14-18 December 2022, Auckland, New Zealand (Proceedings of Machine Learning Research, Vol. 205)*, Karen Liu, Dana Kulic, and Jeffrey Ichnowski (Eds.). PMLR, 287–318. <https://proceedings.mlr.press/v205/ichter23a.html>
- [24] Michael Janner, Yilun Du, Joshua B. Tenenbaum, and Sergey Levine. 2022. Planning with Diffusion for Flexible Behavior Synthesis. In *International Conference on Machine Learning, ICML 2022, 17-23 July 2022, Baltimore, Maryland, USA (Proceedings of Machine Learning Research, Vol. 162)*, Kamalika Chaudhuri, Stefanie Jegelka, Le Song, Csaba Szepesvári, Gang Niu, and Sivan Sabato (Eds.). PMLR, 9902–9915. <https://proceedings.mlr.press/v162/janner22a.html>
- [25] Albert Q. Jiang, Alexandre Sablayrolles, Arthur Mensch, Chris Bamford, Devendra Singh Chaplot, Diego de Las Casas, Florian Bressand, Gianna Lengyel, Guillaume Lample, Lucile Saulnier, Léo Renard Lavaud, Marie-Anne Lachaux, Pierre Stock, Teven Le Scao, Thibaut Lavril, Thomas Wang, Timothée Lacroix, and William El Sayed. 2023. Mistral 7B. *CoRR* abs/2310.06825 (2023). <https://doi.org/10.48550/ARXIV.2310.06825> arXiv:2310.06825
- [26] Tero Karras, Miika Aittala, Timo Aila, and Samuli Laine. 2022. Elucidating the Design Space of Diffusion-Based Generative Models. In *Advances in Neural Information Processing Systems 35: Annual Conference on Neural Information Processing Systems 2022, NeurIPS 2022, New Orleans, LA, USA, November 28 - December 9, 2022*, Sammi Koyejo, S. Mohamed, A. Agarwal, Danielle Belgrave, K. Cho, and A. Oh (Eds.). http://papers.nips.cc/paper_files/paper/2022/hash/a98846e9d9cc01cfb87eb694d946ce6b-Abstract-Conference.html
- [27] Tsung-Wei Ke, Nikolaos Gkanatsios, and Katerina Fragkiadaki. 2024. 3D Diffuser Actor: Policy Diffusion with 3D Scene Representations. *CoRR* abs/2402.10885 (2024). <https://doi.org/10.48550/ARXIV.2402.10885> arXiv:2402.10885
- [28] Alexander Khazatsky, Karl Pertsch, Suraj Nair, Ashwin Balakrishna, Sudeep Dasari, Siddharth Karamcheti, Soroush Nasiriany, Mohan Kumar Srirama, Lawrence Yunliang Chen, Kirsty Ellis, Peter David Fagan, Joey Hejna, Masha Itkina, Marion Lepert, Yecheng Jason Ma, Patrick Tree Miller, Jimmy Wu, Suneel Belkhal, Shivin Dass, Huy Ha, Arhan Jain, Abraham Lee, Youngwoon Lee, Marius Memmel, Sungjae Park, Ilija Radosavovic, Kaiyuan Wang, Albert Zhan, Kevin Black, Cheng Chi, Kyle Beltran Hatch, Shan Lin, Jingpei Lu, Jean Mercat, Abdul Rehman, Pannag R. Sanketi, Archit Sharma, Cody Simpson, Quan Vuong, Homer Rich Walke, Blake Wulfe, Ted Xiao, Jonathan Heewon Yang, Arefeh Yavary, Tony Z. Zhao, Christopher Agia, Rohan Bajjal, Mateo Guaman Castro, Daphne Chen, Qiuyu Chen, Trinity Chung, Jaimyn Drake, Ethan Paul Foster, and et al. 2024. DROID: A Large-Scale In-The-Wild Robot Manipulation Dataset. *CoRR* abs/2403.12945 (2024). <https://doi.org/10.48550/ARXIV.2403.12945> arXiv:2403.12945
- [29] Vitaly Kurin, Sebastian Nowozin, Katja Hofmann, Lucas Beyer, and Bastian Leibe. 2017. The Atari Grand Challenge Dataset. *CoRR* abs/1705.10998 (2017). arXiv:1705.10998 <http://arxiv.org/abs/1705.10998>
- [30] Corey Lynch, Ayzaan Wahid, Jonathan Tompson, Tianli Ding, James Betker, Robert Baruch, Travis Armstrong, and Pete Florence. 2022. Interactive Language: Talking to Robots in Real Time. *CoRR* abs/2210.06407 (2022). <https://doi.org/10.48550/ARXIV.2210.06407> arXiv:2210.06407
- [31] Antoine Miech, Dimitri Zhukov, Jean-Baptiste Alayrac, Makarand Tapaswi, Ivan Laptev, and Josef Sivic. 2019. HowTo100M: Learning a Text-Video Embedding by Watching Hundred Million Narrated Video Clips. In *2019 IEEE/CVF International Conference on Computer Vision, ICCV 2019, Seoul, Korea (South), October 27 - November 2, 2019*. IEEE, 2630–2640. <https://doi.org/10.1109/ICCV.2019.00272>
- [32] Sewon Min, Xinxin Lyu, Ari Holtzman, Mikel Artetxe, Mike Lewis, Hannaneh Hajishirzi, and Luke Zettlemoyer. 2022. Rethinking the Role of Demonstrations: What Makes In-Context Learning Work?. In *Proceedings of the 2022 Conference on Empirical Methods in Natural Language Processing, EMNLP 2022, Abu Dhabi, United Arab Emirates, December 7-11, 2022*, Yoav Goldberg, Zornitsa Kozareva, and Yue Zhang (Eds.). Association for Computational Linguistics, 11048–11064. <https://doi.org/10.18653/v1/2022.emnlp-main.759>
- [33] Abby O'Neill, Abdul Rehman, Abhiram Maddukuri, Abhishek Gupta, Abhishek Padalkar, Abraham Lee, Acorn Pooley, Agrim Gupta, Ajay Mandlekar, Ajinkya Jain, Albert Tung, Alex Bewley, Alexander Herzog, Alex Irpan, Alexander Khazatsky, Anant Rai, Anchit Gupta, Andrew Wang, Anikait Singh, Animesh Garg, Aniruddha Kembhavi, Annie Xie, Anthony Brohan, Antonin Raffin, Archit Sharma, Arefeh Yavary, Arhan Jain, Ashwin Balakrishna, Ayzaan Wahid, Ben Burgess-Limerick, Beomjoon Kim, Bernhard Schölkopf, Blake Wulfe, Brian Ichter, Cewu Lu, Charles Xu, Charlotte Le, Chelsea Finn, Chen Wang, Chenfeng Xu, Cheng Chi, Chenguang Huang, Christine Chan, Christopher Agia, Chuer Pan, Chuyuan Fu, Coline Devin, Danfei Xu, Daniel Morton, Danny Driess, Daphne Chen, Deepak Pathak, Dhruv Shah, Dieter Buechler, Dinesh Jayaraman, Dmitry Kalashnikov, Dorsa Sadigh, Edward Johns, Ethan Paul Foster, Fangchen Liu, Federico Ceola, Fei Xia, Feiyu Zhao, Freek Stulp, Gaoyue Zhou, Gaurav S. Sukhatme, Gautam Salhotra, Ge Yan, Gilbert Feng, Giulio Schiavi, Glen Berseth, Gregory Kahn, Guanzhi Wang, Hao Su, Haoshu Fang, Haochen Shi, Henghui Bao, Heni Ben Amor, Henrik I. Christensen, Hiroki Furuta, Homer Walke, Hongjie Fang, Huy Ha, Igor Mordatch, Ilija Radosavovic, Isabel Leal, Jacky Liang, Jad Abou-Chakra, Jaehyung Kim, Jaimyn Drake, Jan Peters, Jan Schneider, Jasmine Hsu, Jeanette Bohg, Jeffrey Bingham, Jeffrey Wu, Jensen Gao, Jiaheng Hu, Jiajun Wu, Jialin Wu, Jiankai Sun, Jianlan Luo, Jiayuan Gu, Jie Tan, Jihoon Oh, Jimmy Wu, Jingpei Lu, Jingyu Yang, Jitendra Malik, João Silvério, Joey Hejna, Jonathan Booher, Jonathan Tompson, Jonathan Yang, Jordi Salvador, Joseph J. Lim, Junhyek Han, Kaiyuan Wang, Kanishka Rao, Karl Pertsch, Karol Hausman, Keegan Go, Keerthana Gopalakrishnan, Ken Goldberg, Kendra Byrne, Kenneth Oslund, Kento Kawaharazuka, Kevin Black, Kevin Lin, Kevin Zhang, Kiana Ehsani, Kiran Lekkala, Kirsty Ellis, Krishan Rana, Krishnan Srinivasan, Kuan Fang, Kunal Pratap Singh, Kuo-Hao Zeng, Kyle Hatch, Kyle Hsu, Laurent Itti, Lawrence Yunliang Chen, Lerrel Pinto, Li Fei-Fei, Liam Tan, Linxi Jim Fan, Lionel Ott, Lisa Lee, Luca Weihs, Magnus Chen, Marion Lepert, Marius Memmel, Masayoshi Tomizuka, Masha Itkina, Mateo Guaman Castro, Max Pero, Maximilian Du, Michael Ahn, Michael C. Yip, Mingtong Zhang, Mingyu Ding, Minh Ho, Mohan Kumar Srirama, Mohit Sharma, Moo Jin Kim, Naoaki Kanazawa, Nicklas Hansen, Nicolas Heess, Nikhil J. Joshi, Niko Sünderhauf, Ning Liu, Norman Di Palo, Nur Muhammad (Mahi) Shafiqullah, Oier Mees, Olivier Kroemer, Osbert Bastani, Pannag R. Sanketi, Patrick Tree Miller, Patrick Yin, Paul Wohlhart, Peng Xu, Peter David Fagan, Peter Mitran, Pierre Sermanet, Pieter Abbeel, Priya Sundaresan, Qiuyu Chen, Quan Vuong, Rafael Rafailov, Ran Tian, Ria Doshi, Roberto Martin-Martín, Rohan Bajjal, Rosario Scalise, Rose Hendrix, Roy Lin, Runjia Qian, Ruohan Zhang, Russell Mendonca, Rutav Shah, Ryan Hoque, Ryan Julian, Samuel Bustamante, Sean Kirmani, Sergey Levine, Shan Lin, Sherry Moore, Shikhar Bahl, Shivin Dass, Shubham D. Sonawani, Shuran Song, Sichun Xu, Siddhant Haldar, Siddharth Karamcheti, Simeon Adebola, Simon Guist, Soroush Nasiriany, Stefan Schaal, Stefan Welker, Stephen Tian, Subramanian Ramamoorthy, Sudeep Dasari, Suneel Belkhal, Sungjae Park, Suraj Nair, Suvir Mirchandani, Takayuki Osa, Tanmay Gupta, Tatsuya Harada, Tatsuya Matsushima, Ted Xiao, Thomas Kollar, Tianhe Yu, Tianli Ding, Todor Davchev, Tony Z. Zhao, Travis Armstrong, Trevor Darrell, Trinity Chung, Vidhi Jain, Vincent Vanhoucke, Wei Zhan, Wenxuan Zhou, Wolfram Burgard, Xi Chen, Xiaolong Wang, Xinghao Zhu, Xinyang Geng, Xiuyan Liu, Liangwei Xu, Xuanlin Li, Yao Lu, Yecheng Jason Ma, Yejin Kim, Yevgen Chebotar, Yifan Zhou, Yifeng Zhu, Yilin Wu, Ying Xu, Yixuan Wang, Yonatan Bisk, Yoonyoung Cho, Youngwoon Lee, Yuchen Cui, Yue Cao, Yue-Hua Wu, Yujin Tang, Yuke Zhu, Yunchu Zhang, Yunfan Jiang, Yunshuang Li, Yunzhu Li, Yusuke Iwasawa, Yutaka Matsuo, Zehan Ma, Zhuo Xu, Zichen Jeff Cui, Zichen Zhang, and Zipeng Lin. 2024. Open X-Embodiment: Robotic Learning Datasets and RT-X Models : Open X-Embodiment Collaboration. In *IEEE International Conference on Robotics and Automation, ICRA 2024, Yokohama, Japan, May 13-17, 2024*. IEEE, 6892–6903. <https://doi.org/10.1109/ICRA57147.2024.10611477>
- [34] OpenAI. 2023. GPT-4 Technical Report. *CoRR* abs/2303.08774 (2023). <https://doi.org/10.48550/ARXIV.2303.08774> arXiv:2303.08774
- [35] Sungjae Park, Seung-ho Lee, Mingi Choi, Jiye Lee, Jeonghwan Kim, Jisoo Kim, and Hanbyul Joo. 2025. Learning to Transfer Human Hand Skills for Robot Manipulations. *arXiv preprint arXiv:2501.04169* (2025).
- [36] Colin Raffel, Noam Shazeer, Adam Roberts, Katherine Lee, Sharan Narang, Michael Matena, Yanqi Zhou, Wei Li, and Peter J. Liu. 2020. Exploring the Limits of Transfer Learning with a Unified Text-to-Text Transformer. *J. Mach. Learn. Res.* 21 (2020), 140:1–140:67. <https://jmlr.org/papers/v21/20-074.html>
- [37] Scott E. Reed, Konrad Zolna, Emilio Parisotto, Sergio Gómez Colmenarejo, Alexander Novikov, Gabriel Barth-Maron, Mai Gimenez, Yury Sulsky, Jackie Kay, Jost Tobias Springenberg, Tom Eccles, Jake Bruce, Ali Razavi, Ashley Edwards, Nicolas Heess, Yutian Chen, Raia Hadsell, Oriol Vinyals, Mahyar Bordbar, and Nando de Freitas. 2022. A Generalist Agent. *Trans. Mach. Learn. Res.* 2022 (2022). <https://openreview.net/forum?id=1tkK0kHjv>
- [38] Robin Rombach, Andreas Blattmann, Dominik Lorenz, Patrick Esser, and Björn Ommer. 2022. High-Resolution Image Synthesis with Latent Diffusion Models. In *IEEE/CVF Conference on Computer Vision and Pattern Recognition, CVPR 2022, New Orleans, LA, USA, June 18-24, 2022*. IEEE, 10674–10685. <https://doi.org/10.1109/CVPR52688.2022.01042>
- [39] Chitwan Saharia, William Chan, Saurabh Saxena, Lala Li, Jay Wang, Emily L. Denton, Seyed Kamyar Seyed Ghasemipour, Raphael Gontijo Lopes, Burcu Karagol Ayan, Tim Salimans, Jonathan Ho, David J. Fleet, and Mohammad Norouzi. 2022. Photorealistic Text-to-Image Diffusion Models with Deep Language Understanding. In *Advances in Neural Information Processing Systems 35: Annual Conference on Neural Information Processing Systems 2022, NeurIPS 2022, New Orleans, LA, USA, November 28 - December 9, 2022*, Sammi Koyejo, S. Mohamed, A. Agarwal, Danielle Belgrave,

- K. Cho, and A. Oh (Eds.). http://papers.nips.cc/paper_files/paper/2022/hash/ec795aeadae0b7d230fa35c041-Abstract-Conference.html
- [40] Tim Salimans and Jonathan Ho. 2022. Progressive Distillation for Fast Sampling of Diffusion Models. In *The Tenth International Conference on Learning Representations, ICLR 2022, Virtual Event, April 25–29, 2022*. OpenReview.net. <https://openreview.net/forum?id=TiDIXlpzhol>
- [41] Christoph Schuhmann, Richard Vencu, Romain Beaumont, Robert Kaczmarczyk, Clayton Mullis, Aarush Katta, Theo Coombes, Jenia Jitsev, and Aran Komatsuzaki. 2021. LAION-400M: Open Dataset of CLIP-Filtered 400 Million Image-Text Pairs. *CoRR abs/2111.02114* (2021). arXiv:2111.02114 <https://arxiv.org/abs/2111.02114>
- [42] Yang Song, Prafulla Dhariwal, Mark Chen, and Ilya Sutskever. 2023. Consistency Models. In *International Conference on Machine Learning, ICML 2023, 23–29 July 2023, Honolulu, Hawaii, USA (Proceedings of Machine Learning Research, Vol. 202)*, Andreas Krause, Emma Brunskill, Kyunghyun Cho, Barbara Engelhardt, Sivan Sabato, and Jonathan Scarlett (Eds.). PMLR, 32211–32252. <https://proceedings.mlr.press/v202/song23a.html>
- [43] Yang Song and Stefano Ermon. 2019. Generative Modeling by Estimating Gradients of the Data Distribution. In *Advances in Neural Information Processing Systems 32: Annual Conference on Neural Information Processing Systems 2019, NeurIPS 2019, December 8–14, 2019, Vancouver, BC, Canada*, Hanna M. Wallach, Hugo Larochelle, Alina Beygelzimer, Florence d’Alché-Buc, Emily B. Fox, and Roman Garnett (Eds.). 11895–11907. <https://proceedings.neurips.cc/paper/2019/hash/3001ef257407d5a371a96dcd947c7d93-Abstract.html>
- [44] Yang Song, Jascha Sohl-Dickstein, Diederik P. Kingma, Abhishek Kumar, Stefano Ermon, and Ben Poole. 2021. Score-Based Generative Modeling through Stochastic Differential Equations. In *9th International Conference on Learning Representations, ICLR 2021, Virtual Event, Austria, May 3–7, 2021*. OpenReview.net. <https://openreview.net/forum?id=PxTIG12RRHS>
- [45] Octo Model Team, Dibya Ghosh, Homer Walke, Karl Pertsch, Kevin Black, Oier Mees, Sudeep Dasari, Joey Hejna, Tobias Kreiman, Charles Xu, Jianlan Luo, You Liang Tan, Lawrence Yunliang Chen, Pannag Sanketi, Quan Vuong, Ted Xiao, Dorsa Sadigh, Chelsea Finn, and Sergey Levine. 2024. Octo: An Open-Source Generalist Robot Policy. *CoRR abs/2405.12213* (2024). <https://doi.org/10.48550/ARXIV.2405.12213> arXiv:2405.12213
- [46] Daniel Toyama, Philippe Hamel, Anita Gergely, Gheorghe Comanici, Amelia Glaese, Zafarali Ahmed, Tyler Jackson, Shibl Mourad, and Doina Precup. 2021. AndroidEnv: A Reinforcement Learning Platform for Android. *CoRR abs/2105.13231* (2021). arXiv:2105.13231 <https://arxiv.org/abs/2105.13231>
- [47] Ashish Vaswani, Noam Shazeer, Niki Parmar, Jakob Uszkoreit, Llion Jones, Aidan N. Gomez, Lukasz Kaiser, and Illia Polosukhin. 2017. Attention is All you Need. In *Advances in Neural Information Processing Systems 30: Annual Conference on Neural Information Processing Systems 2017, December 4–9, 2017, Long Beach, CA, USA*, Isabelle Guyon, Ulrike von Luxburg, Samy Bengio, Hanna M. Wallach, Rob Fergus, S. V. N. Vishwanathan, and Roman Garnett (Eds.). 5998–6008. <https://proceedings.neurips.cc/paper/2017/hash/3f5ee243547dee91fbd0531c4a845aa-Abstract.html>
- [48] Tianyu Wang, Dwait Bhatt, Xiaolong Wang, and Nikolay Atanasov. 2024. Cross-Embodiment Robot Manipulation Skill Transfer using Latent Space Alignment. *CoRR abs/2406.01968* (2024). <https://doi.org/10.48550/ARXIV.2406.01968> arXiv:2406.01968
- [49] Lucas Weber, Elia Bruni, and Dieuwke Hupkes. 2023. Mind the instructions: a holistic evaluation of consistency and interactions in prompt-based learning. In *Proceedings of the 27th Conference on Computational Natural Language Learning, CoNLL 2023, Singapore, December 6–7, 2023*, Jing Jiang, David Reitter, and Shumin Deng (Eds.). Association for Computational Linguistics, 294–313. <https://doi.org/10.18653/V1/2023.CONLL-1.20>
- [50] Sen Wu, Hongyang R. Zhang, and Christopher Ré. 2020. Understanding and Improving Information Transfer in Multi-Task Learning. In *8th International Conference on Learning Representations, ICLR 2020, Addis Ababa, Ethiopia, April 26–30, 2020*. OpenReview.net. <https://openreview.net/forum?id=SylzhkbtDB>
- [51] Zhiyong Wu, Chengcheng Han, Zichen Ding, Zhenmin Weng, Zhoumianze Liu, Shunyu Yao, Tao Yu, and Lingpeng Kong. 2024. OS-Copilot: Towards Generalist Computer Agents with Self-Improvement. *CoRR abs/2402.07456* (2024). <https://doi.org/10.48550/ARXIV.2402.07456> arXiv:2402.07456
- [52] Mengda Xu, Zhenjia Xu, Cheng Chi, Manuela Veloso, and Shuran Song. 2023. XSkill: Cross Embodiment Skill Discovery. In *Conference on Robot Learning, CoRL 2023, 6–9 November 2023, Atlanta, GA, USA (Proceedings of Machine Learning Research, Vol. 229)*, Jie Tan, Marc Toussaint, and Kourosh Darvish (Eds.). PMLR, 3536–3555. <https://proceedings.mlr.press/v229/xu23a.html>
- [53] Sherry Yang, Ofir Nachum, Yilun Du, Jason Wei, Pieter Abbeel, and Dale Schuurmans. 2023. Foundation Models for Decision Making: Problems, Methods, and Opportunities. *CoRR abs/2303.04129* (2023). <https://doi.org/10.48550/ARXIV.2303.04129> arXiv:2303.04129
- [54] Chenshuang Zhang, Chaoning Zhang, Sheng Zheng, Mengchun Zhang, Maryam Qamar, Sung-Ho Bae, and In So Kweon. 2023. A Survey on Audio Diffusion Models: Text To Speech Synthesis and Enhancement in Generative AI. *CoRR abs/2303.13336* (2023). <https://doi.org/10.48550/ARXIV.2303.13336> arXiv:2303.13336
- [55] Duo Zheng, Shijia Huang, Lin Zhao, Yiwu Zhong, and Liwei Wang. 2024. Towards Learning a Generalist Model for Embodied Navigation. In *IEEE/CVF Conference on Computer Vision and Pattern Recognition, CVPR 2024, Seattle, WA, USA, June 16–22, 2024*. IEEE, 13624–13634. <https://doi.org/10.1109/CVPR52733.2024.01293>
- [56] Yifan Zhong, Jakub Grudzien Kuba, Xidong Feng, Siyi Hu, Jiaming Ji, and Yaodong Yang. 2024. Heterogeneous-Agent Reinforcement Learning. *J. Mach. Learn. Res.* 25 (2024), 32:1–32:67. <https://jmlr.org/papers/v25/zhong24.html>
- [57] Brianna Zitkovich, Tianhe Yu, Sichun Xu, Peng Xu, Ted Xiao, Fei Xia, Jialin Wu, Paul Wohlhart, Stefan Welker, Ayyaan Wahid, Quan Vuong, Vincent Vanhoucke, Huong T. Tran, Radu Soricut, Anikait Singh, Jaspier Singh, Pierre Sermanet, Pannag R. Sanketi, Grecia Salazar, Michael S. Ryoo, Krista Reymann, Kanishka Rao, Karl Pertsch, Igor Mordatch, Henryk Michalewski, Yao Lu, Sergey Levine, Lisa Lee, Tsang-Wei Edward Lee, Isabel Leal, Yuheng Kuang, Dmitry Kalashnikov, Ryan Julian, Nikhil J. Joshi, Alex Irpan, Brian Ichter, Jasmine Hsu, Alexander Herzog, Karol Hausman, Keerthana Gopalakrishnan, Chuyuan Fu, Pete Florence, Chelsea Finn, Kumar Avinava Dubey, Danny Driess, Tianli Ding, Krzysztof Marcin Choro-manski, Xi Chen, Yevgen Chebotar, Justice Carbajal, Noah Brown, Anthony Brohan, Montserrat Gonzalez Arenas, and Kehang Han. 2023. RT-2: Vision-Language-Action Models Transfer Web Knowledge to Robotic Control. In *Conference on Robot Learning, CoRL 2023, 6–9 November 2023, Atlanta, GA, USA (Proceedings of Machine Learning Research, Vol. 229)*, Jie Tan, Marc Toussaint, and Kourosh Darvish (Eds.). PMLR, 2165–2183. <https://proceedings.mlr.press/v229/zitkovich23a.html>

A BABYAI ENVIRONMENT

We adapted the official BabyAI implementation³ to handle a larger range of actions. The complete list of actions can be found in Table 6. We used the BabyAI bot to generate the demonstrations for the different agent types. In Table 7 one can find the the different dataset sizes used for each environment instance.

B TRAINING DETAILS

B.1 Conditional Diffusion Model

We modify the implementation of Karras et al. [26]⁴ to handle the conditioning on the different agent informations presented in Section 3.3. We adopt their hyperparameters of the diffusion process (see Table 8) and keep them constant across all three environments (GoToObj, GoToDistractor, GoToDistractorLarge). For the number of sampling steps we choose 64 as increasing the number of sampling steps did not lead to performance improvements

³<https://github.com/Farama-Foundation/Minigrid>

⁴<https://github.com/NVlabs/edm>

Table 6: The extended action space for the BabyAI environment.

Action ID	Effect
0	Turn left
1	Turn right
2	Move forward
3	Pick up
4	Drop
5	Toggle
6	Done
7	Diagonal Left
8	Diagonal Right
9	Move Right
10	Move Down
11	Move Left
12	Move Up
13	Turn Around
14	Left Diagonal Backwards
15	Right Diagonal Backwards
16	Move Left no turn
17	Move Right no turn
18	Backward

Table 7: Dataset sizes for a single agent dataset that is used for creating the pooled dataset for all three environments. Note that this refers to the number of trajectories contained in the dataset. For the GoToDistractorLarge (GoToDist.-Large) environment the trajectories consists of more timesteps. As a result more instruction-subsequence pairs can be sampled from a single trajectory in the larger environment in comparison to a trajectory from the smaller environments.

Dataset	GoToObj	GoToDist.	GoToDist.-Large
Single Agent	1494	90000	25000

worth the additional computational effort. The training specific hyperparameters for all three environments can be found in Table 9.

B.2 Inverse Dynamics Model

The inverse dynamics model for each agent are trained on the small agent-specific datasets. The input observations are concatenated along the channel dimension and processed by a convolutional block with residual connections. Then mean pooling is applied across all pixels and the resulting embedding is processed via a linear layer. The inverse dynamics model is trained via the cross-entropy loss. The training parameters can be found in Table 10.

B.3 Imitation Learning

We follow the architecture from Hui et al. [22], but remove the LSTM-component since we perform imitation learning in the fully

Table 8: The hyperparameters of the conditional diffusion model adopted from Karras et al. [26]. These values were used for all three environment instances.

Parameter	Value
σ_{min}	0.002
σ_{max}	80
σ_{data}	0.5
ρ	7
P_{mean}	-1.2
P_{std}	1.2
sampling steps	64

Table 9: The training hyperparameters for all three environments. The Hardware used for training the model in the GoToDist. environment was a NVIDIA A100 partitioned into two instances with 20GB each.

Parameter	GoToObj	GoToDist.	GoToDist.-Large
# Updates	500.000	1.000.000	500.000
Learning Rate	0.00002	0.00002	0.00005
Batch-Size	64	128	512
Hardware	NVIDIA TITAN X (Pascal) (12GB)	NVIDIA -A100 (40GB)-MIG	NVIDIA -A100 (40GB)

Table 10: Training parameters for the inverse dynamics models. In case of multiple values, they refer to the values used for the GoToObj, GoToDistractor and GoToDistractorLarge environment respectively.

Parameter	Value
# Epochs	500/10/100
Learning Rate	0.0001
Batch-Size	64 / 64 / 256
Hardware	NVIDIA TITAN X (Pascal)(12GB)

observable variant of the BabyAI environment. The training details for all imitation learning baselines can be found in Table 11. All models were trained until convergence of the action prediction accuracy on the validation dataset.

Table 11: Training parameters for the different imitation learning baselines for the GoToObj and GoToDistractor environment. In case of multiple values they refer to the methods Imitation Learning - Small Single Agent Dataset, Imitation Learning - Large Single Agent Dataset, Imitation Learning - Unione of Action Spaces and Imitation Learning - Agent Heads respectively. Single values indicate that the value is shared across all baselines.

Parameter	GoToObj	GoToDist
# Epochs	100/25/100/25	50/20/30/20
Learning Rate	0.0001	0.0001
Batch-Size	64	128
Hardware	NVIDIA TITAN X (Pascal) (12GB)	NVIDIA TITAN X (Pascal) (12GB)